Convergence results for the local defect correction method as an iterative process

Convergence Results for the Local Defect Correction Method as an Iterative Process

M.J.H. Anthonissen, R.M.M. Mattheij, J.H.M. ten Thije Boonkkamp

Department of Mathematics and Computing Science,
Eindhoven University of Technology,
P.O. Box 513, 5600 MB Eindhoven, The Netherlands,
e-mail: m.j.h.anthonissen@tue.nl

Abstract

We study the local defect correction (LDC) method, introduced in [7]. We focus on the behavior of LDC as an iterative method and derive several useful expressions for the iteration matrix. For the model problem of Poisson's equation on the unit square and standard five-point finite difference discretizations on uniform grids, it is shown via both an upper bound for the norm of the iteration matrix and numerical experiments, that the rate of convergence of the LDC method depends quadratically on H, the grid size of the global, coarse grid. This implies that the rate of convergence of the LDC iteration improves when H tends to zero.

Key words. elliptic problems, local defect correction, composite grids, convergence

AMS subject classifications. 65N22, 65N50

1 Introduction

Many initial boundary value problems produce solutions that have highly localized properties. Examples of partial differential equations (PDEs) with solutions that are rapidly varying functions of the spatial or temporal coordinates appear e.g. in shock hydrodynamics, transport in porous media and combustion processes.

For boundary value problems with solutions that have one or a few small regions with high activity, one needs to have a fine grid in regions with high activity, whereas a coarser grid would suffice in the rest of the domain. Hence, the usage of uniform fine grids is computationally inefficient. A natural choice would be to use a truly nonuniform refined grid. However, uniform grids have several advantages over truly nonuniform grids: uniform grids can be represented by simple data structures, there are simple accurate discretization stencils for uniform grids and there are fast solution techniques for solving the system of equations resulting from discretization on uniform grids. For these reasons, so-called local uniform grid refinement techniques have been introduced in which a coarse base grid covering the whole computational domain is locally uniformly refined.

We consider a discretization method for elliptic boundary value problems in which the discretization on the composite grid is based on a combination of standard discretizations on several uniform grids with different grid sizes that cover different parts of the domain. At least one grid,

the coarse grid, should cover the entire domain, and its grid size should be chosen in agreement with the relatively smooth behavior of the solution outside the high activity areas. Apart from the global, coarse grid, one or several local, fine grids are used which are also uniform. Each of the local grids covers only a (small) part of the domain and contains a high activity region. The grid sizes of the local grids are chosen in agreement with the behavior of the continuous solution in that part of the domain.

In [7], Hackbusch introduced the *local defect correction* (LDC) method for approximating the continuous solution of elliptic boundary value problems on a composite grid. In this method, which is an iterative process, a basic global discretization is improved by local discretizations defined in subdomains. This update of the coarse grid solution is achieved by adding a defect correction term to the right hand side of the coarse grid problem. At each iteration step, the process yields a discrete approximation of the continuous solution on the composite grid. The discrete problem that is actually being solved is an implicit result of the iterative process. Therefore, the LDC method is both a discretization and iterative solution method. An analysis of the LDC technique in combination with finite difference discretizations is presented in [4–6]. The LDC method is combined with finite volume discretizations in [1]; this results in a scheme that features a discrete conservation property for the composite grid approximation.

This paper focuses on the behavior of the LDC algorithm as an iterative method. In his original paper [7], Hackbusch sketches a general strategy for a convergence proof based on interior regularity of the discrete solution on the local fine grid. Ferket [4] derives the system of equations that the fixed point of the LDC iteration satisfies, if it exists. He also gives an expression for the iteration matrix of the LDC iteration, but he does not give bounds for the spectral radius or norm of this matrix. In this paper, we present a new expression for the iteration matrix of the LDC iteration, and we show for a model problem (Poisson's equation on the unit square with one area of refinement) that the norm of the iteration matrix depends quadratically on H, the grid size of the global, coarse grid.

Convergence of the LDC iteration in a finite element context was studied by Wappler [15]. Wappler gives a convergence proof of the LDC iteration in a variational setting. To accomplish his proof, Wappler had to make some restrictive assumptions on the interpolation and restriction operators in the LDC algorithm. Just like in the finite difference context, Wappler finds the rate of convergence of the iteration to improve with the grid size of the coarse grid.

Discretization methods on composite grids have been discussed by other authors. McCormick presents the finite volume element (FVE) method, which is used in the fast adaptive composite grid (FAC) method (cf. [11, 12, 14]). Ewing et al. [2, 3] give an analysis of a finite volume based local refinement technique with composite grids. In both approaches, an explicit discretization scheme for the composite grid is proposed, in which special difference stars near the composite grid interfaces are used. The resulting discrete system is then solved by an iterative method (e.g. FAC) which may take advantage of the composite grid structure. This is a crucial difference with the LDC method, which combines standard discretizations on uniform grids only and does not use an a priori given composite grid discretization. For the FAC method in a variational setting, convergence results have been given by McCormick [9]; the variational theory is extended to the finite volume element method in [10] by interpreting FVE as an approximate finite element scheme.

This paper is organized as follows. In Section 2, we formulate the LDC method for an elliptic boundary value problem that is discretized on a global, coarse grid with one local region of refinement. In Section 3, we prove some simple properties of the LDC algorithm and of the fixed point of the LDC iteration. An expression is derived for the iteration matrix. In Section 4, we consider the algorithm for a model problem, Poisson's equation on the unit square. For the coarse grid discretization, we use the standard five-point stencil for the Laplacian; on the local

region, we solve a continuous boundary value problem. Trigonometric interpolation is used on the interface between the coarse grid and the local region. It is shown that the rate of convergence depends quadratically on H, the grid size of the global, coarse grid, provided we use a safety region that is independent of H. In Section 5, we consider the same model problem as in Section 4, but here we use the standard five-point stencil for the Laplacian on a uniform, fine grid in the local region. We show that the rate of convergence depends quadratically on H, as in Section 4. In Section 6, we verify the theoretical results of Sections 4 and 5 in some numerical experiments.

2 Formulation of the LDC Algorithm

We consider the elliptic boundary value problem

$$\begin{cases} Lu = f, & \text{in } \Omega, \\ u = g, & \text{on } \partial\Omega. \end{cases} \tag{1}$$

In (1), L is a linear, elliptic differential operator, and f and g are the source term and Dirichlet boundary condition, respectively.

To discretize (1), we first choose a global, coarse grid (grid size H), which we denote by Ω^H. An initial approximation u_0^H on Ω^H can be found by solving the system

$$L^H u_0^H = f^H, \tag{2}$$

which is a discretization of boundary value problem (1). In (2), the right hand side f^H incorporates the source term f as well as the Dirichlet boundary condition g. We assume L^H to be invertible.

Although we will not be specific about the elliptic operator L and the discrete operator L^H in this section, it may help to think of them as $L = -\Delta$, and L^H the standard five-point stencil approximating $-\Delta$. Here, Δ denotes the two-dimensional Laplacian operator.

Now, assume that the continuous solution u of (1) has a high activity region in some (small) part of the domain. This high activity of u may be captured by discretizing (1) on a composite grid. To this end, we choose $\Omega_l \subset \Omega$ such that the high activity region of u is contained in Ω_l.

In Ω_l, we choose a local, fine grid (grid size h), which we denote by Ω_l^h. The fine grid is chosen such that $\Omega^H \cap \Omega_l \subset \Omega_l^h$, i.e., grid points of the global, coarse grid that lie in the area of refinement belong to the local, fine grid, too.

The second step of the LDC iteration as described in [7], involves defining artificial boundary conditions on Γ, the interface between Ω_l and $\Omega \setminus \Omega_l$, see Figure 1. We assume that these artificial boundary conditions are found by applying an interpolation operator $P^{h,H}$. The operator $P^{h,H}$ maps function values at grid points of the coarse grid that lie on the interface, notation Γ^H, to function values at grid points of the fine grid that lie on the interface, notation Γ^h. If we denote the vector space of grid functions on Γ^H by $F(\Gamma^H)$, and likewise introduce $F(\Gamma^h)$, we have $P^{h,H} : F(\Gamma^H) \to F(\Gamma^h)$. In practice, we take $P^{h,H}$ to be either linear or quadratic interpolation on the interface. For the proofs in Sections 4 and 5, we assume $P^{h,H}$ to be trigonometric interpolation. This is explained in detail in Section 4.1.

In this way, we find the following approximation $u_{l,0}^h$ on Ω_l^h:

$$L_l^h u_{l,0}^h = f_l^h - B_{l,\Gamma}^h P^{h,H}\left(u_0^H|_\Gamma\right). \tag{3}$$

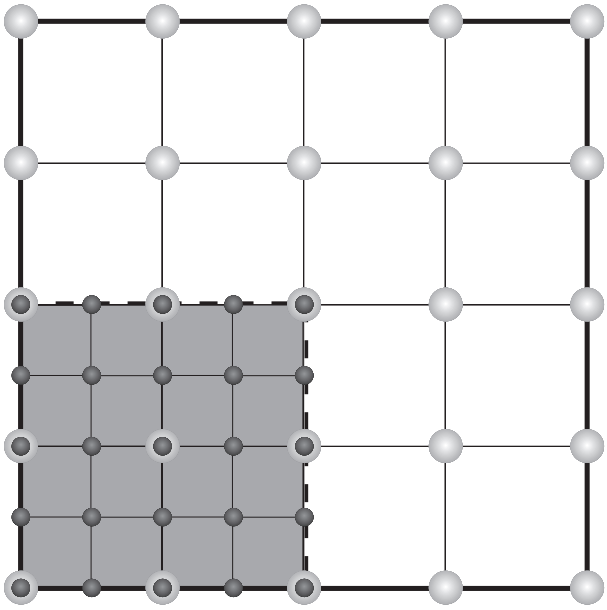

Figure 1: A global coarse and a local fine grid. The darker area is the area of high activity Ω_l. The interface Γ is dashed. Large circles, not located on the domain boundary, are nodes of the coarse grid. Smaller circles, not located on the domain boundary or the interface, are nodes of the local fine grid.

In (3), the matrix L_l^h is a discrete approximation of the differential operator L on the subdomain Ω_l, and the first term of the right hand side f_l^h incorporates the source term f as well as the Dirichlet boundary condition g on $\partial\Omega_l \setminus \Gamma$ given in (1). The dependence on the coarse grid approximation via the artificial Dirichlet boundary condition is made explicit by the second term in the right hand side. We assume L_l^h to be invertible.

Note that the grid points of the coarse grid may be partitioned into three subsets,

$$\Omega^H = \Omega_l^H \cup \Gamma^H \cup \Omega_c^H,$$

where $\Omega_l^H = \Omega^H \cap \Omega_l$, $\Gamma^H = \Omega^H \cap \Gamma$ and $\Omega_c^H = \Omega^H \setminus (\Omega_l^H \cup \Gamma^H)$. See Figure 2.

Using this partitioning of Ω^H, we set

$$u^H = \begin{pmatrix} u_l^H \\ u_\Gamma^H \\ u_c^H \end{pmatrix}.$$

We will apply this same partitioning for other grid functions in $F(\Omega^H)$ too. Assuming that the maximum stencil we use is a nine-point stencil, i.e., the stencil in grid point (x, y) involves (at most) function values at $(x+iH, y+jH)$ with $i, j \in \{-1, 0, 1\}$, we can split the discrete operator L^H as

$$L^H = \begin{pmatrix} L_l^H & B_{l,\Gamma}^H & 0 \\ B_{\Gamma,l}^H & L_\Gamma^H & B_{\Gamma,c}^H \\ 0 & B_{c,\Gamma}^H & L_c^H \end{pmatrix}. \tag{4}$$

In the special case that L equals $-\Delta$ and L^H is the standard five-point stencil, we have $B_{\Gamma,l}^H = (B_{l,\Gamma}^H)^T$ and $B_{\Gamma,c}^H = (B_{c,\Gamma}^H)^T$.

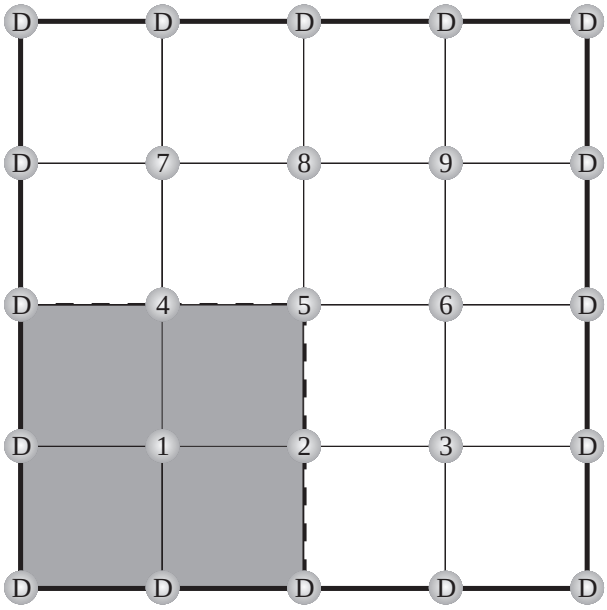

Figure 2: A global coarse grid and its partitioning. The darker area is the area of high activity Ω_l. The interface Γ is dashed. We have $\Omega_l^H = \{1\}$, $\Gamma^H = \{2,4,5\}$, and $\Omega_c^H = \{3,6,7,8,9\}$. Grid points on the boundary are labeled D.

Using this decomposition, the coarse grid initialization (2) may also be written

$$\begin{pmatrix} L_l^H & B_{l,\Gamma}^H & 0 \\ B_{\Gamma,l}^H & L_\Gamma^H & B_{\Gamma,c}^H \\ 0 & B_{c,\Gamma}^H & L_c^H \end{pmatrix} \begin{pmatrix} u_{l,0}^H \\ u_{\Gamma,0}^H \\ u_{c,0}^H \end{pmatrix} = \begin{pmatrix} f_l^H \\ f_\Gamma^H \\ f_c^H \end{pmatrix}. \tag{5}$$

After the first two steps of the algorithm, i.e., one coarse grid solve and one local, fine grid solve, we have found the coarse grid approximations $u_{l,0}^H$, $u_{\Gamma,0}^H$, and $u_{c,0}^H$, and the fine grid approximation $u_{l,0}^h$. We remark that we have one approximation in each grid point (x,y) of Γ^H and Ω_c^H, namely $u_{\Gamma,0}^H(x,y)$ and $u_{c,0}^H(x,y)$, respectively, and that we have two approximations in each grid point (x,y) of Ω_l^H, namely both $u_{l,0}^H(x,y)$ and $u_{l,0}^h(x,y)$. Of these last two approximations, $u_{l,0}^h(x,y)$ is considered to be more accurate, as it is calculated on a finer grid.

In the third step of the LDC algorithm, we try to improve the coarse grid approximation by using the approximation $u_{l,0}^h$ calculated on the local, fine grid to estimate the local truncation error of the coarse grid discretization. For the description of this step, we introduce the operator $R^{H,h} : F(\Omega_l^h) \to F(\Omega_l^H)$ as the restriction from Ω_l^h onto Ω_l^H, viz. $(R^{H,h}u_l^h)(x,y) = u_l^h(x,y)$ for all $u_l^h \in F(\Omega_l^h)$, $(x,y) \in \Omega_l^H$.

If we would substitute the projection on Ω^H of the exact solution u of boundary value problem (1) into the coarse grid discretization (2), we would find the local truncation error or defect d^H, given by

$$L^H\left(u|_{\Omega^H}\right) = f^H + d^H.$$

In particular, we would find the following defect on Ω_l^H:

$$L_l^H\left(u|_{\Omega_l^H}\right) + B_{l,\Gamma}^H\left(u|_{\Gamma^H}\right) = f_l^H + d_l^H. \tag{6}$$

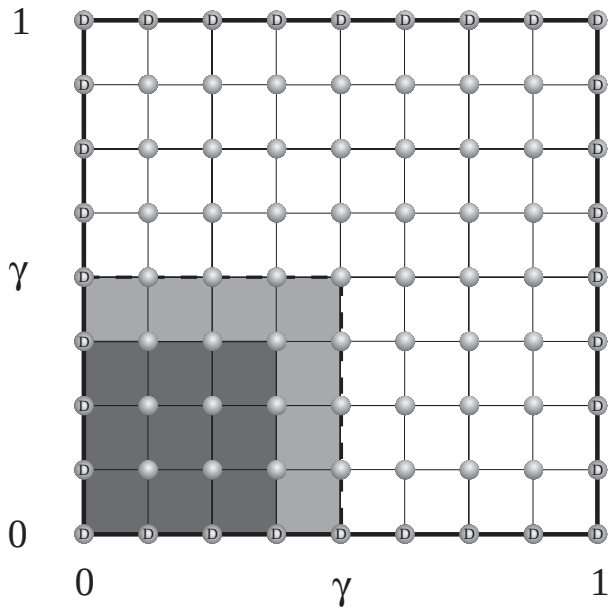

Figure 3: The area of refinement is the union of the light and dark gray areas. The safety region is light gray. The defect is only calculated in grid points lying inside the dark gray area. For this situation, the sets Ω_l^H and Ω_{def}^H consist of nine and four grid points, respectively.

In case we would know the values of the defect d^H, we could use them to find a better approximation on the coarse grid. This could be achieved by putting the defect vector in the right hand side of (2). However, as we do not know the exact solution of the boundary value problem, we can calculate neither d^H nor d_l^H.

What we can do though, is use the approximation $u_{l,0}^h$ calculated on the fine, local grid to estimate d_l^H. Using (6), we find

$$d_l^H = L_l^H\left(u|_{\Omega_l^H}\right) + B_{l,\Gamma}^H\left(u|_{\Gamma^H}\right) - f_l^H \approx L_l^H R^{H,h} u_{l,0}^h + B_{l,\Gamma}^H u_{\Gamma,0}^H - f_l^H =: d_{l,0}^H. \tag{7}$$

Using (7), we find an estimate of the local truncation error of the coarse grid discretization in all points of Ω_l^H. Therefore, we can update the coarse grid approximation by placing the estimate (7) in the right hand side of the coarse grid equation (2) or (5). This leads to the *coarse grid correction step* to find u_i^H, $i = 1$, on the coarse grid

$$L^H u_i^H = \begin{pmatrix} f_l^H + d_{l,i-1}^H \\ f_\Gamma^H \\ f_c^H \end{pmatrix} = \begin{pmatrix} L_l^H R^{H,h} u_{l,i-1}^h + B_{l,\Gamma}^H u_{\Gamma,i-1}^H \\ f_\Gamma^H \\ f_c^H \end{pmatrix}. \tag{8}$$

Previous results [7, 15] show, that it may be beneficial to use the estimate (7) not in all points of Ω_l^H, but in a subset of Ω_l^H only. In particular, nodes in Ω_l^H lying close to the interface Γ should be excluded. This leads to the introduction of what might be called a *safety region*, see Figure 3, in which a subset Ω_{def}^H of Ω_l^H has been chosen.

The estimate for the local truncation error of the coarse grid discretization is placed in the right hand side of equations corresponding to grid points belonging to the set Ω_{def}^H only. This leads to

the following generalization of (8):

$$L^H u_i^H = \begin{pmatrix} f_l^H + X_l^H d_{l,i-1}^H \\ f_\Gamma^H \\ f_c^H \end{pmatrix} = \begin{pmatrix} (I - X_l^H) f_l^H + X_l^H \left(L_l^H R^{H,h} u_{l,i-1}^h + B_{l,\Gamma}^H u_{\Gamma,i-1}^H \right) \\ f_\Gamma^H \\ f_c^H \end{pmatrix}. \quad (9)$$

In (9), we have used $X_l^H : F(\Omega_l^H) \to F(\Omega_l^H)$ which is defined by

$$\left(X_l^H u_l^H\right)(x,y) = \begin{cases} u_l^H(x,y), & (x,y) \in \Omega_{\text{def}}^H \\ 0, & (x,y) \in \Omega_l^H \setminus \Omega_{\text{def}}^H, \end{cases}$$

for all grid functions $u_l^H \in F(\Omega_l^H)$. Note that X_l^H is the matrix corresponding to multiplication of a grid function on Ω_l^H by the characteristic function of Ω_{def}^H. If $\Omega_{\text{def}}^H = \Omega_l^H$, we use the estimate for the truncation error in all points of Ω_l^H, and (9) reduces to (8). If $\Omega_{\text{def}}^H = \emptyset$, we do not use any components of the estimate of the truncation error, and (9) reduces to the initial system (2) or (5). Therefore, the situation $\Omega_{\text{def}}^H = \emptyset$ yields $u_1^H = u_0^H$, and is not of interest; in what follows, we will assume $\Omega_{\text{def}}^H \neq \emptyset$.

Under this assumption, (9) produces a new solution u_1^H on the coarse grid. Because (9) incorporates estimates of the local truncation error of the coarse grid discretization, the new solution u_1^H is assumed to be more accurate than u_0^H. Hence, the new solution u_1^H provides a better boundary condition on the interface Γ, and a better solution on the local fine grid can be found as before (cf. (3)) by solving ($i = 1$)

$$L_l^h u_{l,i}^h = f_l^h - B_{l,\Gamma}^h P^{h,H} u_{\Gamma,i}^H. \quad (10)$$

Summarizing, we have found the following iterative method for solving boundary value problem (1), which we will refer to as the LDC algorithm.

LDC Algorithm

Initialization

- Solve the basic coarse grid problem (2).
- Solve the local, fine grid problem (3).

Iteration, $i = 1, 2, \ldots$

- Solve the updated coarse grid problem (9).
- Solve the local, fine grid problem (10).

In Section 3, we will prove some properties of this algorithm.

3 Properties of the LDC Algorithm

The following lemma shows that once the coarse grid approximations do not change value on the interface, the LDC algorithm converges and the fixed point of the iteration has been reached.

Lemma 1 *If $u^H_{\Gamma,k} = u^H_{\Gamma,k-1}$ for a certain index k, then the LDC iteration (2), (3), (9), (10) converges and it has reached its fixed point, i.e.,*

$$u^H_i = u^H_k, \qquad u^h_{l,i} = u^h_{l,k},$$

for all $i \geq k$.

Proof. Assume that $u^H_{\Gamma,k} = u^H_{\Gamma,k-1}$ for a certain index k. From (10), we have that $u^h_{l,k} = u^h_{l,k-1}$, and hence, from (9),

$$\begin{aligned} L^H u^H_{k+1} &= \begin{pmatrix} (I - X^H_l) f^H_l + X^H_l \left(L^H_l R^{H,h} u^h_{l,k} + B^H_{l,\Gamma} u^H_{\Gamma,k} \right) \\ f^H_\Gamma \\ f^H_c \end{pmatrix} \\ &= \begin{pmatrix} (I - X^H_l) f^H_l + X^H_l \left(L^H_l R^{H,h} u^h_{l,k-1} + B^H_{l,\Gamma} u^H_{\Gamma,k-1} \right) \\ f^H_\Gamma \\ f^H_c \end{pmatrix} = L^H u^H_k. \end{aligned}$$

Because we have assumed L^H to be invertible, we have $u^H_{k+1} = u^H_k$ for all grid points in the global, coarse grid. As $\Gamma^H \subset \Omega^H$, we have $u^H_{\Gamma,k+1} = u^H_{\Gamma,k}$. By induction, we find $u^H_i = u^H_k$ and $u^h_{l,i} = u^h_{l,k}$ for all $i \geq k$. □

The equations describing the iteration, (9), (10), can be written in matrix notation as

$$\begin{aligned} &\begin{pmatrix} L^h_l & 0 & B^h_{l,\Gamma} P^{h,H} & 0 \\ 0 & L^H_l & B^H_{l,\Gamma} & 0 \\ 0 & B^H_{\Gamma,l} & L^H_\Gamma & B^H_{\Gamma,c} \\ 0 & 0 & B^H_{c,\Gamma} & L^H_c \end{pmatrix} \begin{pmatrix} u^h_{l,i} \\ u^H_{l,i} \\ u^H_{\Gamma,i} \\ u^H_{c,i} \end{pmatrix} \\ &= \begin{pmatrix} 0 & 0 & 0 & 0 \\ X^H_l L^H_l R^{H,h} & 0 & X^H_l B^H_{l,\Gamma} & 0 \\ 0 & 0 & 0 & 0 \\ 0 & 0 & 0 & 0 \end{pmatrix} \begin{pmatrix} u^h_{l,i-1} \\ u^H_{l,i-1} \\ u^H_{\Gamma,i-1} \\ u^H_{c,i-1} \end{pmatrix} + \begin{pmatrix} f^h_l \\ (I - X^H_l) f^H_l \\ f^H_\Gamma \\ f^H_c \end{pmatrix}. \end{aligned} \tag{11}$$

We will use the following short notation for (11):

$$L^{H,h} u^{H,h}_i = S^{H,h} u^{H,h}_{i-1} + \tilde{f}^{H,h}. \tag{12}$$

If the LDC algorithm converges, then this equation has a fixed point, which we will denote by

$$u^{H,h} = \begin{pmatrix} u^h_l \\ u^H_l \\ u^H_\Gamma \\ u^H_c \end{pmatrix},$$

where the same the partitioning is used as above. The fixed point $u^{H,h}$ satisfies, by definition,

$$L^{H,h} u^{H,h} = S^{H,h} u^{H,h} + \tilde{f}^{H,h}. \tag{13}$$

For the LDC algorithm without a safety region, the fixed point $u^{H,h}$ has the following nice properties.

Theorem 2 *Consider the LDC iteration (2), (3), (9), (10) for the special case that there is no safety region, i.e., $\Omega^H_{def} = \Omega^H_l$, $X^H_l = I$. If the LDC iteration converges, then the fixed point $u^{H,h}$ of the iteration (12) has the following two properties:*

- *the projection of* u_l^h *on the local coarse grid equals* u_l^H*, viz.*

$$R^{H,h} u_l^h = u_l^H,$$

- u_l^h, u_Γ^H, *and* u_c^H *satisfy the system of equations*

$$\begin{pmatrix} L_l^h & B_{l,\Gamma}^h P^{h,H} & 0 \\ B_{\Gamma,l}^H R^{H,h} & L_\Gamma^H & B_{\Gamma,c}^H \\ 0 & B_{c,\Gamma}^H & L_c^H \end{pmatrix} \begin{pmatrix} u_l^h \\ u_\Gamma^H \\ u_c^H \end{pmatrix} = \begin{pmatrix} f_l^h \\ f_\Gamma^H \\ f_c^H \end{pmatrix}. \tag{14}$$

Proof. From (13), we find

$$\left(L^{H,h} - S^{H,h}\right) u^{H,h} = \tilde{f}^{H,h}.$$

Substituting the matrices $L^{H,h}$ and $S^{H,h}$ and using $X_l^H = I$ gives

$$\begin{pmatrix} L_l^h & 0 & B_{l,\Gamma}^h P^{h,H} & 0 \\ -L_l^H R^{H,h} & L_l^H & 0 & 0 \\ 0 & B_{\Gamma,l}^H & L_\Gamma^H & B_{\Gamma,c}^H \\ 0 & 0 & B_{c,\Gamma}^H & L_c^H \end{pmatrix} \begin{pmatrix} u_l^h \\ u_l^H \\ u_\Gamma^H \\ u_c^H \end{pmatrix} = \begin{pmatrix} f_l^h \\ 0 \\ f_\Gamma^H \\ f_c^H \end{pmatrix}. \tag{15}$$

The second equation of this system reads

$$-L_l^H R^{H,h} u_l^h + L_l^H u_l^H = 0,$$

which gives the first claim. Elimination of u_l^H from (15) gives (14). □

Introducing the iteration error of the LDC method by

$$e_i^{H,h} = u_i^{H,h} - u^{H,h},$$

and subtracting (12) and (13), we are led to the following equation for successive iteration errors

$$L^{H,h} e_i^{H,h} = S^{H,h} e_{i-1}^{H,h}.$$

Note that the convergence behavior of the LDC algorithm does not depend on the source term and Dirichlet boundary condition. Using the definitions of $L^{H,h}$ and $S^{H,h}$, see (11), (12), we find:

$$\begin{pmatrix} L_l^h & 0 & B_{l,\Gamma}^h P^{h,H} & 0 \\ 0 & L_l^H & B_{l,\Gamma}^H & 0 \\ 0 & B_{\Gamma,l}^H & L_\Gamma^H & B_{\Gamma,c}^H \\ 0 & 0 & B_{c,\Gamma}^H & L_c^H \end{pmatrix} \begin{pmatrix} e_{l,i}^h \\ e_{l,i}^H \\ e_{\Gamma,i}^H \\ e_{c,i}^H \end{pmatrix} = \begin{pmatrix} 0 \\ X_l^H L_l^H R^{H,h} e_{l,i-1}^h + X_l^H B_{l,\Gamma}^H e_{\Gamma,i-1}^H \\ 0 \\ 0 \end{pmatrix}. \tag{16}$$

The first equation of this system yields

$$e_{l,i}^h = -\left(L_l^h\right)^{-1} B_{l,\Gamma}^h P^{h,H} e_{\Gamma,i}^H. \tag{17}$$

Replacing i with $i-1$ in (17), we can reformulate the last three equations in system (16) as:

$$\begin{pmatrix} L_l^H & B_{l,\Gamma}^H & 0 \\ B_{\Gamma,l}^H & L_\Gamma^H & B_{\Gamma,c}^H \\ 0 & B_{c,\Gamma}^H & L_c^H \end{pmatrix} \begin{pmatrix} e_{l,i}^H \\ e_{\Gamma,i}^H \\ e_{c,i}^H \end{pmatrix} = \begin{pmatrix} -X_l^H L_l^H R^{H,h} \left(L_l^h\right)^{-1} B_{l,\Gamma}^h P^{h,H} e_{\Gamma,i-1}^H + X_l^H B_{l,\Gamma}^H e_{\Gamma,i-1}^H \\ 0 \\ 0 \end{pmatrix},$$

or, equivalently,

$$L^H e_i^H = \begin{pmatrix} I \\ 0 \\ 0 \end{pmatrix} X_l^H \left(B_{l,\Gamma}^H - L_l^H R^{H,h} \left(L_l^h \right)^{-1} B_{l,\Gamma}^h P^{h,H} \right) e_{\Gamma,i-1}^H. \tag{18}$$

This leads to the following theorem.

Theorem 3 *The behavior of the LDC algorithm as an iterative method is fully described by the following iteration on the interface only ($i = 1, 2, \ldots$)*

$$e_{\Gamma,i}^H = M e_{\Gamma,i-1}^H, \tag{19}$$

in which the iteration matrix $M : F(\Gamma^H) \to F(\Gamma^H)$ is defined by

$$M = (0\ I\ 0) \left(L^H \right)^{-1} \begin{pmatrix} I \\ 0 \\ 0 \end{pmatrix} X_l^H \left[B_{l,\Gamma}^H - L_l^H R^{H,h} \left(L_l^h \right)^{-1} B_{l,\Gamma}^h P^{h,H} \right]. \tag{20}$$

As before, $e_{\Gamma,i}^H$ is the difference of the successive coarse grid approximations $u_{\Gamma,i}^H$ on the interface with the fixed point values u_Γ^H on the interface.

Proof. It is easily verified, that (18) gives (19). Equation (19) describes the behavior of component $e_{\Gamma,i}^H$ of the iteration error; the other components of the iteration error can be expressed in $e_{\Gamma,i}^H$ by (17) and (18). Therefore, if we can prove that $e_{\Gamma,i}^H \to 0$ ($i \to \infty$), it follows that $e_i^{H,h} \to 0$ ($i \to \infty$), which means that the LDC algorithm converges to a fixed point. □

Expression (20) for the iteration matrix differs from the expressions by Hackbusch [7, Sec. 3.3.1], and Ferket [4, Th. 3.9], and is believed to be new. From Theorem 3, we conclude that we can prove convergence of the LDC algorithm by showing that the spectral radius of the iteration matrix M is less than one. It is sufficient to show that the norm of M is less than one in some matrix norm. This will be the topic of the next sections.

4 Estimate of the Norm of the Iteration Matrix for a Continuous Local Problem

In this section, we estimate the infinity norm of the iteration matrix M from Theorem 3 for a model problem with special choices of the grids and discretizations in the LDC algorithm. We will prove convergence results for the Poisson problem on the unit square, viz.

$$\begin{cases} -\Delta u = f, & \text{in } \Omega = (0,1)^2, \\ u = g, & \text{on } \partial\Omega. \end{cases} \tag{21}$$

We choose the computational grid Ω^H to be a uniform grid with grid sizes $\Delta x = \Delta y = H$, $N := 1/H$ integer:

$$\Omega^H = \{(lH, jH) \mid l = 1, 2, \ldots, N-1,\ j = 1, 2, \ldots, N-1\}. \tag{22}$$

Furthermore, we let L^H be the standard five-point discretization of the Laplacian on Ω^H. We take the area of high activity Ω_l to be $\Omega_l = (0,\gamma)^2$, $0 < \gamma < 1$, with γ a multiple of H. As before, $\Omega_l^H = \Omega^H \cap \Omega_l$.

In this section, we will replace L_l^h by $-\Delta$, the continuous Laplacian on Ω_l. This corresponds to letting $h \to 0$. Of course, L_l^h will normally be a discrete operator, and we will take L_l^h to be discrete in Section 5. We choose $L_l^h = -\Delta$ in this section, because this simplifies the analysis significantly whereas the estimate for the norm of the iteration matrix will show the same behavior as the estimate in Section 5. For the interpolation operator $P^{h,H}$ on the interface, we will use trigonometric interpolation; this is explained in Section 4.1. The reason for using this special type of interpolation will become apparent in Section 4.2. Finally, we will need to use a safety region in the LDC algorithm to be able to prove convergence. In particular, we will choose

$$\Omega_{\text{def}}^H = \left\{ (x,y) \in \Omega_l^H \;\middle|\; x < \gamma - \epsilon \;\wedge\; y < \gamma - \epsilon \right\}, \tag{23}$$

with $\epsilon > 0$, ϵ independent of H.

We split the iteration matrix M from Theorem 3 according to

$$M = M_1 M_2,$$

where

$$M_1 = (0\ I\ 0)\left(L^H\right)^{-1}\begin{pmatrix} I \\ 0 \\ 0 \end{pmatrix}, \qquad M_2 = X_l^H\left[B_{l,\Gamma}^H - L_l^H R^{H,h}\left(L_l^h\right)^{-1} B_{l,\Gamma}^h P^{h,H}\right]. \tag{24}$$

Most of the effort will concentrate on establishing an estimate of the norm of M_2, because

$$\|M\|_\infty \le \|M_1\|_\infty \|M_2\|_\infty \le \frac{1}{8}\|M_2\|_\infty. \tag{25}$$

The last inequality is a well-known result for the infinity norm of the discrete Laplacian, see, e.g., [8, Sec. 4.4].

The final result we will establish in the next sections is Theorem 9. This theorem states that under the above assumptions, the iteration matrix M from Theorem 3 satisfies

$$\|M\|_\infty \le CH^2,$$

with C independent of H. This upper bound for the norm of the iteration matrix implies, that the norm of M can become arbitrarily small when the grid size H of the coarse grid tends to zero. Note that this result holds for the LDC algorithm with a safety region only.

4.1 Trigonometric Interpolation

We assume $P^{h,H}$ to be interpolation by a trigonometric polynomial. Consider the interval $(0,\gamma)$ with $\gamma = kH$, k a positive integer, and define the nodes $x_j = jH$, $j = 0,1,\ldots,k$. Let function values g_j, $j = 0,1,\ldots,k$, be given with $g_0 = g_k = 0$. As an interpolating function on $(0,\gamma)$, we will use the trigonometric polynomial g, defined by

$$g(x) = \sum_{m=1}^{k-1} \alpha_m \sin\left(\frac{m\pi x}{\gamma}\right), \qquad x \in (0,\gamma). \tag{26}$$

The right hand side of (26) is a finite Fourier sine series. The coefficients α_m, $m = 1, 2, \ldots, k-1$, follow from the system of equations

$$g(x_j) = g_j = \sum_{m=1}^{k-1} \alpha_m \sin\left(\frac{m\pi x_j}{\gamma}\right), \qquad j = 1, 2, \ldots, k-1.$$

Introducing the matrix A and vectors a, b by

$$A = \begin{pmatrix} \sin(\pi x_1/\gamma) & \sin(2\pi x_1/\gamma) & \cdots & \sin((k-1)\pi x_1/\gamma) \\ \sin(\pi x_2/\gamma) & \sin(2\pi x_2/\gamma) & \cdots & \sin((k-1)\pi x_2/\gamma) \\ \vdots & \vdots & \ddots & \vdots \\ \sin(\pi x_{k-1}/\gamma) & \sin(2\pi x_{k-1}/\gamma) & \cdots & \sin((k-1)\pi x_{k-1}/\gamma) \end{pmatrix},$$

$$a = (\alpha_1, \alpha_2, \ldots, \alpha_{k-1})^T,$$

$$b = (g_1, g_2, \ldots, g_{k-1})^T,$$

the system of equations (4.1) can also be written as $A\,a = b$. In this way, we find

$$a = A^{-1} b.$$

The set of functions

$$\sin\left(\frac{m\pi x}{\gamma}\right), \qquad m = 1, 2, \ldots, k-1,$$

satisfies discrete orthogonality relations, see e.g. [13, Satz 4.4, p. 147]. From these relations, it follows that the matrix A is orthogonal, as stated in the following theorem.

Theorem 4 *The matrix A^{-1} may be expressed in terms of A as*

$$A^{-1} = \frac{2H}{\gamma} A = \frac{2}{k} A.$$

Proof. See [13, Ch. 4]. □

Corollary 5 *For the 2-norm and the infinity norm of A^{-1}, we have*

$$\|A^{-1}\|_2 = \sqrt{\frac{2}{k}}, \qquad \|A^{-1}\|_\infty < \sqrt{2}.$$

Proof. The matrix

$$\tilde{A} = \sqrt{\frac{2}{k}}\, A,$$

is symmetric and, by Theorem 4, orthonormal. Therefore

$$\|A^{-1}\|_2 = \sqrt{\frac{2}{k}}\, \|\tilde{A}^{-1}\|_2 = \sqrt{\frac{2}{k}}.$$

A straightforward estimate gives

$$\|A^{-1}\|_\infty \le \sqrt{k-1}\, \|A^{-1}\|_2 \le \sqrt{\frac{k-1}{k}}\sqrt{2} < \sqrt{2}.$$

This proves the corollary. □

4.2 Estimate for the Case of Non-Zero Artificial Dirichlet Boundary Conditions on the Horizontal Part of the Interface

In this section, we will derive an estimate for the infinity norm of M_2. Note that $M_2 : F(\Gamma^H) \to F(\Omega_l^H)$. To estimate the infinity norm of M_2, we let g_Γ^H be an arbitrary vector in $F(\Gamma^H)$ and split the vector g_Γ^H in

$$g_\Gamma^H = g_{hor}^H + g_{vert}^H + g_{corner}^H. \tag{27}$$

Here, the definitions of g_{hor}^H, g_{vert}^H, and g_{corner}^H are as one would expect:

$$g_{hor}^H(x,y) = \begin{cases} g_\Gamma^H(x,y), & (x,y) \in \Gamma_{hor}^H := \{(lH,\gamma) \mid l = 1,2,\dots,k-1\}, \\ 0, & (x,y) \in \Gamma^H \setminus \Gamma_{hor}^H, \end{cases}$$

$$g_{vert}^H(x,y) = \begin{cases} g_\Gamma^H(x,y), & (x,y) \in \Gamma_{vert}^H := \{(\gamma,jH) \mid j = 1,2,\dots,k-1\}, \\ 0, & (x,y) \in \Gamma^H \setminus \Gamma_{vert}^H, \end{cases}$$

$$g_{corner}^H(x,y) = \begin{cases} g_\Gamma^H(x,y), & (x,y) = (\gamma,\gamma), \\ 0, & (x,y) \in \Gamma^H \setminus \{(\gamma,\gamma)\}. \end{cases}$$

For the moment, we will assume, that both g_{vert}^H and g_{corner}^H equal zero. Hence, we will only give an estimate of $\|M_2 g_{hor}^H\|_\infty$. In the next sections, we will treat the cases of non-zero g_{vert}^H and g_{corner}^H. It will turn out, that the estimate of the term $\|M_2 g_{vert}^H\|_\infty$ is analogous to the estimate given in this section; the treatment of a non-zero corner value is more involved and is discussed in Section 4.4.

From the definition of M_2, see (24), we have

$$M_2 g_{hor}^H = X_l^H \left[B_{l,\Gamma}^H g_{hor}^H + L_l^H R^{H,h} u_{hor} \right], \tag{28}$$

where

$$u_{hor} = -\left(L_l^h\right)^{-1} B_{l,\Gamma}^h P^{h,H} g_{hor}^H.$$

In view of the definitions of L_l^h, $B_{l,\Gamma}^h$, and $P^{h,H}$, it follows that u_{hor} is the solution of the boundary value problem

$$\begin{cases} \Delta u_{hor} = 0, & \text{in } \Omega_l, \\ u_{hor} = g_{hor}, & \text{on } \Gamma, \\ u_{hor} = 0, & \text{on } \partial\Omega_l \setminus \Gamma. \end{cases} \tag{29}$$

In (29), $g_{hor} = P^{h,H} g_{hor}^H$ vanishes on the vertical part of the interface Γ, i.e., $g_{hor}(\gamma,y) = 0$ for $y \in (0,\gamma)$. The function g_{hor} is the trigonometric polynomial interpolating g_{hor}^H on the horizontal part of the interface. Hence, $g_{hor}(x,\gamma)$ has the form (26) for $x \in (0,\gamma)$, and its coefficients α_m, $m = 1,2,\dots,k-1$, satisfy (cf. Corollary 5)

$$|\alpha_m| < \sqrt{2}\,\|g_{hor}^H\|_\infty, \qquad m = 1,2,\dots,k-1. \tag{30}$$

Due to the specific form of g_{hor}, the exact solution of boundary value problem (29) is readily seen to be

$$u_{hor}(x,y) = \sum_{m=1}^{k-1} \alpha_m \sin(m\pi x/\gamma)\, \frac{\sinh(m\pi y/\gamma)}{\sinh(m\pi)}, \qquad (x,y) \in \Omega_l. \tag{31}$$

Equation (28) states, that $M_2 g^H_{hor}(x,y)$ equals the residual of the standard five-point stencil for the Laplacian applied to the function u_{hor} in (x,y) for all grid points $(x,y) \in \Omega^H_{def}$. For this reason, we find

$$\begin{aligned}\left(M_2 g^H_{hor}\right)(x,y) = -\frac{1}{H^2}\big[&u_{hor}(x+H,y) - 2u_{hor}(x,y) + u_{hor}(x-H,y)\\ &+ u_{hor}(x,y+H) - 2u_{hor}(x,y) + u_{hor}(x,y-H)\big].\end{aligned} \tag{32}$$

Using the equalities

$$\sin\left(\frac{m\pi(x+H)}{\gamma}\right) - 2\sin\left(\frac{m\pi x}{\gamma}\right) + \sin\left(\frac{m\pi(x-H)}{\gamma}\right) = -4\sin^2\left(\frac{m\pi H}{2\gamma}\right)\sin\left(\frac{m\pi x}{\gamma}\right),$$

$$\sinh\left(\frac{m\pi(y+H)}{\gamma}\right) - 2\sinh\left(\frac{m\pi y}{\gamma}\right) + \sinh\left(\frac{m\pi(y-H)}{\gamma}\right) = 4\sinh^2\left(\frac{m\pi H}{2\gamma}\right)\sinh\left(\frac{m\pi y}{\gamma}\right),$$

we find the following expression for $\left(M_2 g^H_{hor}\right)(x,y)$:

$$\left(M_2 g^H_{hor}\right)(x,y) = -\frac{4}{H^2}\sum_{m=1}^{k-1}\alpha_m\delta_m \sin\left(m\pi x/\gamma\right)\frac{\sinh(m\pi y/\gamma)}{\sinh(m\pi)}. \tag{33}$$

Here, δ_m is defined by

$$\delta_m = \sinh^2\left(\frac{m\pi H}{2\gamma}\right) - \sin^2\left(\frac{m\pi H}{2\gamma}\right).$$

We give an estimate for $|\delta_m|$ in the following lemma.

Lemma 6 *For $|\delta_m|$, the following upper bound holds:*

$$|\delta_m| \le CH^4\left(\frac{m\pi}{\gamma}\right)^4,$$

with C independent of H.

Proof. Consider the function f defined by

$$f(x) = \sinh^2 x - \sin^2 x.$$

Developing the function in a Taylor expansion around 0, we find

$$f(x) = \frac{x^4}{4!}f^{(4)}(\xi), \qquad \xi \in (0,x), \qquad f^{(4)}(x) = 8(\cosh^2 x + \sinh^2 x - \cos^2 x + \sin^2 x).$$

Because

$$\delta_m = f\left(\frac{m\pi H}{2\gamma}\right) = \frac{1}{4!}\left(\frac{m\pi H}{2\gamma}\right)^4 f^{(4)}(\xi), \qquad \xi \in (0,\pi/2),$$

and for all $x \in (0,\pi/2)$

$$|f^{(4)}(x)| \le 8\left(\cosh^2(\pi/2) + \sinh^2(\pi/2) + 1\right),$$

we find the following upper bound for $|\delta_m|$

$$|\delta_m| \le \frac{H^4}{48}\left(\frac{m\pi}{\gamma}\right)^4\left[\cosh^2(\pi/2) + \sinh^2(\pi/2) + 1\right] = CH^4\left(\frac{m\pi}{\gamma}\right)^4,$$

with C independent of H. □

From (33), we find by (30) and Lemma 6:

$$\left|\left(M_2 g^H_{\rm hor}\right)(x,y)\right| \le 4CH^2\sqrt{2}\,\|g^H_{\rm hor}\|_\infty \sum_{m=1}^{k-1}\left(\frac{m\pi}{\gamma}\right)^4 \frac{\sinh(m\pi y/\gamma)}{\sinh(m\pi)}. \tag{34}$$

Note that this upper bound depends on H, $\|g^H_{\rm hor}\|_\infty$, γ, and y only (the upper limit of the sum, $k-1$, is a function of γ and H, because $k = \gamma/H$). We will show that we can give an upper bound for the sum in the right hand side of (34) which *does not depend on* H. This implies, that

$$\left\|M_2 g^H_{\rm hor}\right\|_\infty \le C_1 H^2 \|g^H_{\rm hor}\|_\infty.$$

To establish the H-independent upper bound for the sum, we use the assumption made at the start of this section, that $y < \gamma - \epsilon$ with ϵ independent of H. For the sum in (34), we find

$$\sum_{m=1}^{k-1}\left(\frac{m\pi}{\gamma}\right)^4 \frac{\sinh(m\pi y/\gamma)}{\sinh(m\pi)} \le \sum_{m=1}^{\infty}\left(\frac{m\pi}{\gamma}\right)^4 \frac{\sinh(m\pi y/\gamma)}{\sinh(m\pi)} < \infty. \tag{35}$$

Convergence of the series in (35) can be shown using d'Alembert's theorem. Consider the series

$$\sum_{m=1}^{\infty} a_m, \qquad a_m = \left(\frac{m\pi}{\gamma}\right)^4 \frac{\sinh(m\pi y/\gamma)}{\sinh(m\pi)}. \tag{36}$$

We have

$$\begin{aligned}\frac{\sinh(m\pi y/\gamma)}{\sinh(m\pi)} &= \frac{\exp(m\pi y/\gamma) - \exp(-m\pi y/\gamma)}{\exp(m\pi) - \exp(-m\pi)} \\ &= \exp(m\pi(y/\gamma - 1))\,\frac{1-\exp(-2m\pi y/\gamma)}{1-\exp(-2m\pi)},\end{aligned} \tag{37}$$

so that

$$\begin{aligned}\frac{a_{m+1}}{a_m} &= \left(\frac{m+1}{m}\right)^4 \exp(\pi(y/\gamma - 1))\,\frac{1-\exp(-2(m+1)\pi y/\gamma)}{1-\exp(-2m\pi y/\gamma)}\,\frac{1-\exp(-2m\pi)}{1-\exp(-2(m+1)\pi)} \\ &\to \exp\left(\pi\left(\frac{y}{\gamma} - 1\right)\right), \qquad m \to \infty.\end{aligned} \tag{38}$$

For $(x,y) \in \Omega^H_{\rm def}$, we have $y < \gamma - \epsilon$, and we find

$$\exp\left(\pi\left(\frac{y}{\gamma} - 1\right)\right) < \exp\left(\pi\left(\frac{\gamma-\epsilon}{\gamma} - 1\right)\right) < 1, \tag{39}$$

which proves the convergence claimed in (35).

We have now shown that for all $(x,y) \in \Omega^H_{\rm def}$

$$\left|\left(M_2 g^H_{\rm hor}\right)(x,y)\right| \le C_1 H^2 \|g^H_{\rm hor}\|_\infty, \tag{40}$$

with C_1 independent of H.

The results of this section are summarized in the following lemma.

Lemma 7 *Consider the LDC algorithm for the Poisson problem (21) with the following settings. Let* L^H *be the standard five-point discretization of the Laplacian on a uniform grid with grid sizes* $\Delta x = \Delta y = H$ *as in (22). Let* $\Omega_l = (0,\gamma)^2$ *with* $0 < \gamma < 1$ *and* γ *a multiple of* H*. Let* L_l^h *be the continuous Laplacian on* Ω_l*. Let* $P^{h,H}$ *be interpolation by a trigonometric polynomial. Finally, let*

$$\Omega_{def}^H = \left\{ (x,y) \in \Omega_l^H \,\middle|\, x < \gamma - \epsilon \ \wedge \ y < \gamma - \epsilon \right\},$$

for some $\epsilon > 0$*,* ϵ *independent of* H*. Then*

$$\|M_2 g_\Gamma^H\|_\infty \leq C_1 H^2 \|g_\Gamma^H\|_\infty, \tag{41}$$

for all $g_\Gamma^H \in F(\Gamma^H)$ *with* $g_\Gamma^H(x,y) \neq 0$ *for* $(x,y) \in \Gamma_{hor}^H$ *only. In (41),* C_1 *is independent of* H*.*

This lemma concludes the analysis of this section. Lemma 7 is the largest part of establishing the upper bound for the norm of the iteration matrix M of the LDC algorithm. The lemma will be generalized in the next sections by lifting the assumption that $g_\Gamma^H(x,y) \neq 0$ for $(x,y) \in \Gamma_{\text{hor}}^H$ only.

Note that the use of a safety region corresponds to the concept of interior regularity used by Hackbusch [7] and Wappler [15].

4.3 Estimate for the Case of Non-Zero Artificial Dirichlet Boundary Conditions on the Vertical Part of the Interface

Starting from (27), we may also assume, that g_{hor}^H and g_{corner}^H equal zero. Analogous to Section 4.2, we can prescribe artificial Dirichlet boundary conditions $g_{\text{vert}} = P^{h,H} g_{\text{vert}}^H$ by using interpolation with a trigonometric polynomial on the vertical part of the interface. The function g_{vert} vanishes on the horizontal part of the interface. This leads to a local boundary value problem similar to (29). Hence, an analogue of the estimate in Section 4.2 holds. The lemma corresponding to Lemma 7 is the following.

Lemma 8 *Consider the LDC algorithm for the Poisson problem (21) with the following settings. Let* L^H *be the standard five-point discretization of the Laplacian on a uniform grid with grid sizes* $\Delta x = \Delta y = H$ *as in (22). Let* $\Omega_l = (0,\gamma)^2$ *with* $0 < \gamma < 1$ *and* γ *a multiple of* H*. Let* L_l^h *be the continuous Laplacian on* Ω_l*. Let* $P^{h,H}$ *be interpolation by a trigonometric polynomial. Finally, let*

$$\Omega_{def}^H = \left\{ (x,y) \in \Omega_l^H \,\middle|\, x < \gamma - \epsilon \ \wedge \ y < \gamma - \epsilon \right\},$$

for some $\epsilon > 0$*,* ϵ *independent of* H*. Then*

$$\|M_2 g_\Gamma^H\|_\infty \leq C_2 H^2 \|g_\Gamma^H\|_\infty, \tag{42}$$

for all $g_\Gamma^H \in F(\Gamma^H)$ *with* $g_\Gamma^H(x,y) \neq 0$ *for* $(x,y) \in \Gamma_{vert}^H$ *only. In (42),* C_2 *is independent of* H*.*

4.4 Treatment of Artificial Dirichlet Boundary Conditions that are Non-Zero at the Corner of the Interface

In the previous sections, we have used trigonometric interpolation on the interface. However, thus far we have assumed that the artificial Dirichlet boundary conditions equal zero at the corner of the interface, and hence we have defined the interpolation operator $P^{h,H}$ for vectors $g_\Gamma^H \in$

$F(\Gamma^H)$ with $g_\Gamma^H(\gamma,\gamma)$ equal to zero only. If $g_\Gamma^H(\gamma,\gamma) \neq 0$, we proceed as follows. The idea is to subtract a suitable grid function to accomplish a zero corner value. Consider the function

$$v(x,y) = \frac{xy}{\gamma^2}, \qquad (x,y) \in \Omega_l. \tag{43}$$

The function v is linear on the horizontal and the vertical part of the interface Γ, and $v(\gamma,\gamma) = 1$. Furthermore, v vanishes on $\partial\Omega_l \setminus \Gamma$, and v is harmonic in Ω_l. Also, the projection of v on Ω^H is discretely harmonic. For $g_\Gamma^H \in F(\Gamma^H)$ with $g_\Gamma^H(\gamma,\gamma) \neq 0$, we introduce $\tilde{g}_\Gamma^H \in F(\Gamma^H)$ by

$$\tilde{g}_\Gamma^H = g_\Gamma^H - g_\Gamma^H(\gamma,\gamma) \cdot v|_{\Gamma^H}. \tag{44}$$

The grid function $\tilde{g}_\Gamma^H$ is zero in the corner (γ,γ) of the interface. Hence, we can split $\tilde{g}_\Gamma^H$ according to, cf. (27),

$$\tilde{g}_\Gamma^H = \tilde{g}_{hor}^H + \tilde{g}_{vert}^H,$$

and use trigonometric interpolation on both the horizontal and the vertical part of the interface to find artificial Dirichlet boundary conditions $\tilde{g}_{hor}$, $\tilde{g}_{vert}$, respectively. We use the following definition for the interpolation operator $P^{h,H}$:

$$P^{h,H} g_\Gamma^H = \tilde{g}_{hor} + \tilde{g}_{vert} + g_\Gamma^H(\gamma,\gamma) \cdot v|_\Gamma. \tag{45}$$

Using this definition, we have

$$M_2 g_\Gamma^H = M_2 \tilde{g}_{hor}^H + M_2 \tilde{g}_{vert}^H + g_\Gamma^H(\gamma,\gamma) \cdot M_2\left(v|_{\Gamma^H}\right) = M_2 \tilde{g}_{hor}^H + M_2 \tilde{g}_{vert}^H. \tag{46}$$

The last equality holds, because the projection of v is discretely harmonic on the coarse, local grid Ω_l^H. For the remaining two terms in the right hand side, we have the estimates from Sections 4.2 and 4.3. This leads to the main theorem.

Theorem 9 *Consider the LDC algorithm for the Poisson problem (21) with the following settings. Let* L^H *be the standard five-point discretization of the Laplacian on a uniform grid with grid sizes* $\Delta x = \Delta y = H$ *as in (22). Let* $\Omega_l = (0,\gamma)^2$ *with* $0 < \gamma < 1$ *and* γ *a multiple of* H. *Let* L_l^h *be the continuous Laplacian on* Ω_l. *Let* $P^{h,H}$ *be trigonometric interpolation. Finally, let*

$$\Omega_{def}^H = \left\{ (x,y) \in \Omega_l^H \,\middle|\, x < \gamma - \epsilon \ \wedge\ y < \gamma - \epsilon \right\},$$

for some $\epsilon > 0$, ϵ *independent of* H. *Then the following upper bound for the norm of the iteration matrix* M *of the LDC algorithm holds:*

$$\|M\|_\infty \leq CH^2,$$

with C *independent of* H.

Proof. Let $g_\Gamma^H \in F(\Gamma^H)$. Define $\tilde{g}_\Gamma^H \in F(\Gamma^H)$ as in (44). Using (46) and Lemmas 7, 8, we find

$$\|M_2 g_\Gamma^H\|_\infty = \|M_2 \tilde{g}_{hor}^H + M_2 \tilde{g}_{vert}^H\|_\infty \leq (C_1 + C_2) H^2 \|\tilde{g}_\Gamma^H\|_\infty,$$

with C_1, C_2, independent of H. From the definition of $\tilde{g}_\Gamma^H$, it follows that $\|\tilde{g}_\Gamma^H\|_\infty \leq 2\|g_\Gamma^H\|_\infty$, and hence

$$\|M_2\|_\infty \leq 2(C_1 + C_2) H^2.$$

Using (25), we conclude that

$$\|M\|_\infty \leq \frac{1}{4}(C_1 + C_2) H^2 = CH^2,$$

with C independent of H. □

5 Estimate of the Norm of the Iteration Matrix for a Discrete Local Problem

In Section 4, we derived an $\mathcal{O}(H^2)$ upper bound for the iteration matrix of the LDC algorithm with a safety region. One of the assumptions in Section 4 was that the local problem was a continuous boundary value problem. In other words, we assumed h to be equal to zero. In this section, we will drop this assumption and give an upper bound for the iteration matrix for positive values of h.

Hence, we consider the same boundary value problem (21) as in Section 4. As before, we choose the computational grid Ω^H to be a uniform grid with grid sizes $\Delta x = \Delta y = H$, $N := 1/H$ integer, as in (22), and we let L^H be the standard five-point discretization of the Laplacian on Ω^H. We take the area of high activity Ω_l to be $\Omega_l = (0,\gamma)^2$, $0 < \gamma < 1$, with γ a multiple of H.

In this section, we choose a uniform grid Ω_l^h in Ω_l with grid size $\Delta x = \Delta y = h$, $n := \gamma/h$ integer:

$$\Omega_l^h = \{(lh, jh) \mid l = 1, 2, \ldots, n-1,\ j = 1, 2, \ldots, n-1\}. \tag{47}$$

We assume the refinement factor $\sigma := H/h$ to be integer. We let L_l^h be the standard five-point discretization of the Laplacian on Ω_l^h. For the interpolation operator $P^{h,H}$ on the interface, we will use trigonometric interpolation as before. Like in Section 4, we will need to use a safety region in the LDC algorithm to be able to prove convergence, and we will choose Ω_{def}^H as in (23). Again, the analysis will focus on the matrix M_2, cf. (24), (25).

The final result we will establish in the next sections is Theorem 14. This theorem states that under the above assumptions, the iteration matrix M from Theorem 3 satisfies

$$\|M\|_\infty \leq CH^2,$$

with C independent of H. This theorem is the discrete analogon of Theorem 9, the main result of Section 4. Note that this result holds for the LDC algorithm with a safety region only.

5.1 Estimate for the Case of Non-Zero Artificial Dirichlet Boundary Conditions on the Horizontal Part of the Interface

As in Section 4.2, we assume $g_\Gamma^H \in F(\Gamma^H)$ to be given, and we first consider the case where both g_{vert}^H and g_{corner}^H equal zero, cf. (27). Hence, we will only give an estimate of $\|M_2 g_{\text{hor}}^H\|_\infty$. In the next sections, we will treat the cases of non-zero g_{vert}^H and g_{corner}^H. It will turn out, that the estimate of the term $\|M_2 g_{\text{vert}}^H\|_\infty$ is analogous to the estimate given in this section; the treatment of a non-zero corner value is more involved and is discussed in Section 5.3. As in Section 4.2, we use trigonometric interpolation to find artificial Dirichlet boundary conditions g_{hor}^h on the horizontal part of the interface.

From the definition of M_2, see (24), we have

$$M_2 g_{\text{hor}}^H = X_l^H \left[B_{l,\Gamma}^H g_{\text{hor}}^H + L_l^H R^{H,h} u_{\text{hor}}^h \right], \tag{48}$$

where

$$u_{\text{hor}}^h = -\left(L_l^h\right)^{-1} B_{l,\Gamma}^h P^{h,H} g_{\text{hor}}^H. \tag{49}$$

In view of the definitions of L_l^h, $B_{l,\Gamma}^h$, and $P^{h,H}$, it follows that u_{hor}^h satisfies a discrete equivalent of (29); u_{hor}^h satisfies the discrete Laplace equation, viz.

$$\begin{aligned} &u_{hor}^h(x+h,y) - 2u_{hor}^h(x,y) + u_{hor}^h(x-h,y) \\ &+ u_{hor}^h(x,y+h) - 2u_{hor}^h(x,y) + u_{hor}^h(x,y-h) = 0, \end{aligned} \tag{50}$$

in each grid point $(x,y) \in \Omega_l^h$. Artificial Dirichlet boundary conditions $P^{h,H} g_{hor}^H$ are prescribed on the interface Γ; on the horizontal part of Γ, trigonometric interpolation is used, on the vertical part of Γ, the artificial Dirichlet boundary conditions vanish. Dirichlet conditions on $\partial\Omega_l \setminus \Gamma$ vanish, too.

Just as for the continuous boundary value problem, we try the separation of variables technique to find u_{hor}^h. So, we set

$$u_{hor}^h(lh, jh) = X_l Y_j, \qquad l, j = 0, 1, \ldots, n.$$

Substitution into (50) and division by $X_l Y_j$ yields

$$\frac{X_{l+1} - 2X_l + X_{l-1}}{X_l} + \frac{Y_{j+1} - 2Y_j + Y_{j-1}}{Y_j} = 0.$$

We conclude that

$$\frac{X_{l+1} - 2X_l + X_{l-1}}{X_l} = -\frac{Y_{j+1} - 2Y_j + Y_{j-1}}{Y_j} = \mu,$$

with μ, the separation constant, independent of l and j. Standard techniques for solving the recurrence relation for X_l, viz.

$$X_{l+1} - (2+\mu)X_l + X_{l-1} = 0, \tag{51}$$

with boundary conditions $X_0 = X_n = 0$ show, that non-trivial solutions X_l exist for

$$\mu_m = -4\sin^2\left(\frac{m\pi}{2n}\right), \tag{52}$$

in which $m = 1, 2, \ldots, n-1$, with corresponding solutions

$$X_l = \sin\left(\frac{m\pi(lh)}{\gamma}\right), \qquad l = 0, 1, \ldots, n. \tag{53}$$

Note that these solutions are simply the projections of the continuous solutions on the grid, cf. (31). In a similar way, the recurrence relation for Y_j, viz.

$$Y_{j+1} - (2-\mu)Y_j + Y_{j-1} = 0, \tag{54}$$

with boundary conditions $Y_0 = 0$, $Y_n = 1$, has the solutions

$$Y_j = \frac{\sinh(\beta_m j/n)}{\sinh\beta_m} = \frac{\sinh(\beta_m(jh)/\gamma)}{\sinh\beta_m}, \qquad j = 0, 1, \ldots, n, \tag{55}$$

in which the coefficients β_m are defined by

$$\beta_m := 2n\,\mathrm{Arsinh}\left(\sin\left(\frac{m\pi}{2n}\right)\right) = \frac{2\gamma}{h}\,\mathrm{Arsinh}\left(\sin\left(\frac{m\pi h}{2\gamma}\right)\right). \tag{56}$$

The solutions (53) and (55) can be verified by the reader by simple substitution. Notice the similarity between (55) and the solutions $Y(y) = \sinh(m\pi y/\gamma)/\sinh(m\pi)$, $y \in (0,\gamma)$, of the continuous problem, cf. (31), especially as we have

$$\lim_{h\to 0}\beta_m = \lim_{h\to 0}\frac{2\gamma}{h}\,\mathrm{Arsinh}\left(\sin\left(\frac{m\pi h}{2\gamma}\right)\right) = m\pi.$$

Summarizing, the separation of variables method produces the solution

$$u^h_{hor}(lh, jh) = \sum_{m=1}^{k-1} \alpha_m \sin(m\pi(lh)/\gamma) \frac{\sinh(\beta_m(jh)/\gamma)}{\sinh \beta_m}. \tag{57}$$

in which the coefficients α_m follow from the boundary conditions g^h_{hor} on the horizontal part of Γ^h. For $h \to 0$, (57) reduces to the solution (31) of the continuous boundary value problem (29).

Note that $u^h_{hor} = -\left(L^h_l\right)^{-1} B^h_{l,\Gamma} P^{h,H} g^H_{hor}$, and hence

$$\left(M_2 g^H_{hor}\right)(x,y) = \left(B^H_{l,\Gamma} g^H_{hor} + L^H_l R^{H,h} u^h_{hor}\right)(x,y)$$

equals the residual of the standard five-point stencil for the Laplacian applied to u^h_{hor} in the (coarse) grid point $(x,y) \in \Omega^H_{def}$. In a similar way as in Section 4.2, cf. (32), (33), we find the following expression for $\left(M_2 g^H_{hor}\right)(x,y)$:

$$\left(M_2 g^H_{hor}\right)(x,y) = -\frac{4}{H^2} \sum_{m=1}^{k-1} \alpha_m \delta_m \sin(m\pi x/\gamma) \frac{\sinh(\beta_m y/\gamma)}{\sinh \beta_m}. \tag{58}$$

Here, δ_m is defined by

$$\delta_m = \sinh^2\left(\frac{\beta_m H}{2\gamma}\right) - \sin^2\left(\frac{m\pi H}{2\gamma}\right).$$

We give an estimate for $|\delta_m|$ in the following lemma, which is the discrete equivalent of Lemma 6.

Lemma 10 *For $|\delta_m|$, the following upper bound holds:*

$$|\delta_m| \le \left[C_1 H^2 + D_1 h^2\right] H^2 \left(\frac{m\pi}{\gamma}\right)^4,$$

with C_1, D_1, independent of H and h.

Proof. To prove the lemma, we will use some Taylor expansions. From (56), we have

$$\beta_m = \frac{2\gamma}{h} f_1\left(\frac{m\pi h}{2\gamma}\right), \qquad f_1(x) = \operatorname{Arsinh}(\sin x).$$

A simple first order expansion gives

$$\beta_m = \frac{2\gamma}{h} \frac{m\pi h}{2\gamma} f_1'(\xi) = m\pi f_1'(\xi),$$

with $\xi \in (0, m\pi h/(2\gamma)) \subset (0, \pi/2)$. Because

$$f_1'(x) = \frac{\cos x}{\sqrt{1+\sin^2 x}},$$

we have $f_1'(\xi) \in (0,1)$, and hence

$$0 \le \beta_m \le m\pi, \qquad m = 1, 2, \ldots, k-1. \tag{59}$$

Expanding f_1 up to third order, we find

$$f_1(x) = x + \frac{x^3}{3!} f_1^{(3)}(\xi), \qquad \xi \in (0,x), \quad f_1^{(3)}(x) = \frac{-4\sqrt{2}(\cos x + \cos(3x))}{(3-\cos(2x))^{5/2}},$$

and

$$\beta_m = \frac{2\gamma}{h}\left[\frac{m\pi h}{2\gamma} + \frac{1}{3!}\left(\frac{m\pi h}{2\gamma}\right)^3 f_1^{(3)}(\xi_1)\right] = m\pi + \frac{\gamma}{24}\left(\frac{m\pi}{\gamma}\right)^3 h^2 f_1^{(3)}(\xi_1). \tag{60}$$

Next, we define

$$f_2(x) = \sinh^2 x,$$

with Taylor expansion

$$f_2(x) = x^2 + \frac{x^4}{4!}f_2^{(4)}(\xi), \qquad \xi \in (0,x), \quad f_2^{(4)}(x) = 8(\cosh^2 x + \sinh^2 x).$$

Substitution of (60) in the expansion of f_2 yields

$$\begin{aligned}\sinh^2\left(\frac{\beta_m H}{2\gamma}\right) &= \left(\frac{\beta_m H}{2\gamma}\right)^2 + \frac{1}{4!}\left(\frac{\beta_m H}{2\gamma}\right)^4 f_2^{(4)}(\xi_2)\\ &= \frac{H^2}{4}\left(\frac{m\pi}{\gamma}\right)^2 + \frac{H^4}{384}\left(\frac{\beta_m}{\gamma}\right)^4 f_2^{(4)}(\xi_2)\\ &\quad + \frac{H^2h^2}{48}\left(\frac{m\pi}{\gamma}\right)^4 f_1^{(3)}(\xi_1) + \frac{H^2h^4}{2304}\left(\frac{m\pi}{\gamma}\right)^6 \left(f_1^{(3)}(\xi_1)\right)^2.\end{aligned} \tag{61}$$

Finally, we introduce the function

$$f_3(x) = \sin^2 x,$$

which has the Taylor expansion

$$f_3(x) = x^2 + \frac{x^4}{4!}f_3^{(4)}(\xi), \qquad \xi \in (0,x), \quad f_3^{(4)}(x) = 8(\sin^2 x - \cos^2 x).$$

Using this expansion, we find

$$\sin^2\left(\frac{m\pi H}{2\gamma}\right) = \frac{H^2}{4}\left(\frac{m\pi}{\gamma}\right)^2 + \frac{H^4}{384}\left(\frac{m\pi}{\gamma}\right)^4 f_3^{(4)}(\xi_3). \tag{62}$$

Combining (61) and (62), we find the following expression for δ_m:

$$\begin{aligned}\delta_m &= \frac{H^4}{384}\left(\frac{\beta_m}{\gamma}\right)^4 f_2^{(4)}(\xi_2) - \frac{H^4}{384}\left(\frac{m\pi}{\gamma}\right)^4 f_3^{(4)}(\xi_3)\\ &\quad + \frac{H^2h^2}{48}\left(\frac{m\pi}{\gamma}\right)^4 f_1^{(3)}(\xi_1) + \frac{H^2h^4}{2304}\left(\frac{m\pi}{\gamma}\right)^6 \left(f_1^{(3)}(\xi_1)\right)^2.\end{aligned}$$

Note that $\xi_1, \xi_2, \xi_3 \in (0, \pi/2)$, and

$$|f_1^{(3)}(x)| \le 2, \qquad |f_2^{(4)}(x)| \le 8(\cosh^2(\pi/2) + \sinh^2(\pi/2)), \qquad |f_3^{(4)}(x)| \le 8,$$

for all $x \in (0, \pi/2)$. Setting $C := 8(\cosh^2(\pi/2) + \sinh^2(\pi/2))$ and using (59), we have

$$|\delta_m| \le \frac{(C+8)H^4}{384}\left(\frac{m\pi}{\gamma}\right)^4 + \frac{H^2h^2}{24}\left(\frac{m\pi}{\gamma}\right)^4 + \frac{H^2h^4}{576}\left(\frac{m\pi}{\gamma}\right)^6.$$

Because $mH \le \gamma$, we have

$$H^2h^4\left(\frac{m\pi}{\gamma}\right)^6 = H^2h^2\left(\frac{m\pi}{\gamma}\right)^4\left(\frac{m\pi H}{\gamma}\right)^2\frac{1}{\sigma^2} \le H^2h^2\left(\frac{m\pi}{\gamma}\right)^4\left(\frac{\pi}{\sigma}\right)^2,$$

and we can incorporate the third term in the second one; this results in

$$|\delta_m| \leq \left[C_1 H^2 + D_1 h^2\right] H^2 \left(\frac{m\pi}{\gamma}\right)^4,$$

with C_1, D_1, independent of H and h. □

From (58), we find by (30) and Lemma 10:

$$\left|\left(M_2 g_{\text{hor}}^H\right)(x,y)\right| \leq 4\sqrt{2}\left[C_1 H^2 + D_1 h^2\right] \|g_{\text{hor}}^H\|_\infty \sum_{m=1}^{k-1} \left(\frac{m\pi}{\gamma}\right)^4 \frac{\sinh(\beta_m y/\gamma)}{\sinh \beta_m}. \tag{63}$$

Equation (63) is an upper bound that depends on H, h, γ, and y (the upper limit of the sum, $k-1$, is a function of γ and H, because $k = \gamma/H$). For $h \to 0$, one can show that (63) reduces to (34).

We will show that we can give an upper bound for the sum in the right hand side of (63) which *does not depend on* H *or* h. This implies, that $\left|\left(M_2 g_{\text{hor}}^H\right)(x,y)\right|$ is $\mathcal{O}(H^2) + \mathcal{O}(h^2)$. To establish the grid size independent upper bound for the sum, the analysis is a little more subtle than in Section 4.2, as we now have terms with $\sinh(\beta_m y/\gamma)/\sinh\beta_m$ in the sum, whereas we had terms with $\sinh(m\pi y/\gamma)/\sinh(m\pi)$ in Section 4.2. As in Section 4.2, we assume that the value of y is smaller than γ and does not depend on H. This implies, that we consider LDC with a safety region.

We first prove the following lemma.

Lemma 11 *For β_m, $m = 1, 2, \ldots, k-1$, as defined by (56), we have*

$$\beta_{m+1} \geq \beta_m + \frac{1}{3}\pi\sqrt{3}.$$

Proof. Define the function f by

$$f(x) = \operatorname{Arsinh}(\sin x).$$

Then

$$f'(x) = \frac{\cos x}{\sqrt{1+\sin^2 x}},$$

and hence

$$\beta_{m+1} = \frac{2\gamma}{h} f\left(\frac{(m+1)\pi h}{2\gamma}\right) = \frac{2\gamma}{h}\left[f\left(\frac{m\pi h}{2\gamma}\right) + \frac{\pi h}{2\gamma}\cdot f'(\xi)\right] = \beta_m + \pi f'(\xi). \tag{64}$$

In (64), $\xi \in (m\pi h/(2\gamma), (m+1)\pi h/(2\gamma))$. Because $1 \leq m \leq k-1$, we have $\xi \in (0, \pi/(2\sigma))$. If $\sigma = 1$, we have the uninteresting situation that $h = H$ in the LDC algorithm. It is easy to show that the iteration matrix equals the zero matrix in this case. Therefore, we assume $\sigma \geq 2$. This implies that $\xi \in (0, \pi/4)$. For these values of ξ, we have $f'(\xi) \geq \sqrt{3}/3$. With (64), this proves the lemma. □

We have

$$\lim_{h\to 0} \beta_1 = \pi,$$

and hence β_1 is larger than, say, $\pi/2$ for h small enough. We introduce the minorizing sequence $\tilde{\beta}_m$ by

$$\begin{aligned}\tilde{\beta}_1 &= \frac{\pi}{2},\\ \tilde{\beta}_{m+1} &= \tilde{\beta}_m + \frac{1}{3}\pi\sqrt{3}, \qquad m = 1,2,\ldots\end{aligned}$$

Due to Lemma 11 and the definition of the sequence $\tilde{\beta}_m$, $m = 1,2,\ldots$, we have $\beta_m \geq \tilde{\beta}_m$, and hence

$$\sum_{m=1}^{k-1}\left(\frac{m\pi}{\gamma}\right)^4 \frac{\sinh(\beta_m y/\gamma)}{\sinh\beta_m} \leq \sum_{m=1}^{k-1}\left(\frac{m\pi}{\gamma}\right)^4 \frac{\sinh(\tilde{\beta}_m y/\gamma)}{\sinh\tilde{\beta}_m} \leq \sum_{m=1}^{\infty}\left(\frac{m\pi}{\gamma}\right)^4 \frac{\sinh(\tilde{\beta}_m y/\gamma)}{\sinh\tilde{\beta}_m} < \infty.$$

The first inequality holds, because the function

$$f_a(z) = \frac{\sinh(az)}{\sinh z},$$

is decreasing in z for $0 < a < 1$ and $z > 0$. Convergence of the infinite series can again be shown by applying d'Alembert's theorem as in Section 4.3. Define

$$\tilde{a}_m = \left(\frac{m\pi}{\gamma}\right)^4 \frac{\sinh(\tilde{\beta}_m y/\gamma)}{\sinh\tilde{\beta}_m}.$$

We have

$$\frac{\sinh(\tilde{\beta}_m y/\gamma)}{\sinh\tilde{\beta}_m} = \exp\left(\tilde{\beta}_m\left(\frac{y}{\gamma}-1\right)\right)\frac{1-\exp(-2\tilde{\beta}_m y/\gamma)}{1-\exp(-2\tilde{\beta}_m)},$$

and therefore

$$\begin{aligned}\frac{\tilde{a}_{m+1}}{\tilde{a}_m} &= \frac{\exp(\tilde{\beta}_{m+1}(y/\gamma-1))}{\exp(\tilde{\beta}_m(y/\gamma-1))}\frac{1-\exp(-2\tilde{\beta}_{m+1}y/\gamma)}{1-\exp(-2\tilde{\beta}_m y/\gamma)}\frac{1-\exp(-2\tilde{\beta}_m)}{1-\exp(-2\tilde{\beta}_{m+1})}\\ &\to \exp\left(\frac{1}{3}\pi\sqrt{3}\left(\frac{y}{\gamma}-1\right)\right), \qquad m\to\infty. \end{aligned} \tag{65}$$

Because

$$\exp\left(\frac{1}{3}\pi\sqrt{3}\left(\frac{y}{\gamma}-1\right)\right) < 1,$$

we conclude that we can give an upper bound for the sum in (63), that does not depend on H.

We have now shown, that for all $(x,y) \in \Omega^H_{\text{def}}$

$$\left|\left(M_2 g^H_{\text{hor}}\right)(x,y)\right| \leq (C_1 H^2 + D_1 h^2)\,\|g^H_{\text{hor}}\|_\infty, \tag{66}$$

with C_1, D_1, independent of H and h.

The results of this section are summarized in the following lemma, which is the discrete equivalent of Lemma 7.

Lemma 12 *Consider the LDC algorithm for the Poisson problem (21) with the following settings. Let L^H be the standard five-point discretization of the Laplacian on a uniform grid with grid sizes $\Delta x = \Delta y = H$ as in (22). Let $\Omega_1 = (0,\gamma)^2$ with $0 < \gamma < 1$ and γ a multiple of H. Let L^h_1 be the standard five-point*

discretization of the Laplacian on a uniform grid with grid sizes $\Delta x = \Delta y = h$ *as in (47). Let* $P^{h,H}$ *be interpolation by a trigonometric polynomial. Finally, let*

$$\Omega_{def}^H = \left\{ (x,y) \in \Omega_l^H \,\middle|\, x < \gamma - \epsilon \ \wedge \ y < \gamma - \epsilon \right\},$$

for some $\epsilon > 0$, ϵ *independent of* H. *Then*

$$\|M_2 g_\Gamma^H\|_\infty \leq (C_1 H^2 + D_1 h^2)\, \|g_\Gamma^H\|_\infty, \tag{67}$$

for all $g_\Gamma^H \in F(\Gamma^H)$ *with* $g_\Gamma^H(x,y) \neq 0$ *for* $(x,y) \in \Gamma_{hor}^H$ *only. In (67),* C_1 *and* D_1 *are independent of* H *and* h.

5.2 Estimate for the Case of Non-Zero Artificial Dirichlet Boundary Conditions on the Vertical Part of the Interface

Starting from (27), we may also assume, that g_{hor}^H and g_{corner}^H equal zero. Analogous to Section 5.1, we can prescribe artificial Dirichlet boundary conditions g_{vert}^h by using interpolation with a trigonometric polynomial. Now, the non-zero boundary conditions are prescribed on the vertical part of the interface. This leads to equivalents of (49) and (50). Hence, an analogue of the estimate in Section 5.1 holds. The lemma corresponding to Lemma 12 is the following.

Lemma 13 *Consider the LDC algorithm for the Poisson problem (21) with the following settings. Let* L^H *be the standard five-point discretization of the Laplacian on a uniform grid with grid sizes* $\Delta x = \Delta y = H$ *as in (22). Let* $\Omega_l = (0,\gamma)^2$ *with* $0 < \gamma < 1$ *and* γ *a multiple of* H. *Let* L_l^h *be the standard five-point discretization of the Laplacian on a uniform grid with grid sizes* $\Delta x = \Delta y = h$ *as in (47). Let* $P^{h,H}$ *be interpolation by a trigonometric polynomial. Finally, let*

$$\Omega_{def}^H = \left\{ (x,y) \in \Omega_l^H \,\middle|\, x < \gamma - \epsilon \ \wedge \ y < \gamma - \epsilon \right\},$$

for some $\epsilon > 0$, ϵ *independent of* H. *Then*

$$\|M_2 g_\Gamma^H\|_\infty \leq (C_2 H^2 + D_2 h^2)\, \|g_\Gamma^H\|_\infty, \tag{68}$$

for all $g_\Gamma^H \in F(\Gamma^H)$ *with* $g_\Gamma^H(x,y) \neq 0$ *for* $(x,y) \in \Gamma_{vert}^H$ *only. In (68),* C_2 *and* D_2 *are independent of* H *and* h.

5.3 Treatment of Artificial Dirichlet Boundary Conditions that are Non-Zero at the Corner of the Interface

If a vector $g_\Gamma^H \in F(\Gamma^H)$ is such that g_{corner}^H is not equal to zero, then we can subtract a suitable grid function to accomplish a zero corner value as we did in Section 4.4. In fact, the same function as before, cf. (43),

$$v(x,y) = \frac{xy}{\gamma^2}, \qquad (x,y) \in \Omega_l, \tag{69}$$

can be used. We introduce $\tilde{g}_\Gamma^H \in F(\Gamma^H)$ for each vector $g_\Gamma^H \in F(\Gamma^H)$ with $g_\Gamma^H(\gamma,\gamma) \neq 0$ by (cf. (44))

$$\tilde{g}_\Gamma^H = g_\Gamma^H - g_\Gamma^H(\gamma,\gamma) \cdot v|_{\Gamma^H}. \tag{70}$$

The grid function $\tilde{g}_\Gamma^H$ is zero in the corner (γ,γ) of the interface. Hence, we can split $\tilde{g}_\Gamma^H$ according to, cf. (27),

$$\tilde{g}_\Gamma^H = \tilde{g}_{\text{hor}}^H + \tilde{g}_{\text{vert}}^H,$$

and use trigonometric interpolation on both the horizontal and the vertical part of the interface to find artificial Dirichlet boundary conditions $\tilde{g}_{\text{hor}}^h$, $\tilde{g}_{\text{vert}}^h$, respectively. Similar to Section 4.4, we define, cf. (45),

$$P^{h,H} g_\Gamma^H = \tilde{g}_{\text{hor}}^h + \tilde{g}_{\text{vert}}^h + g_\Gamma^H(\gamma,\gamma)\cdot v|_{\Gamma^h}.$$

Using this definition, we have

$$M_2 g_\Gamma^H = M_2\tilde{g}_{\text{hor}}^H + M_2\tilde{g}_{\text{vert}}^H + g_\Gamma^H(\gamma,\gamma)\cdot M_2\left(v|_{\Gamma^H}\right) = M_2\tilde{g}_{\text{hor}}^H + M_2\tilde{g}_{\text{vert}}^H. \tag{71}$$

The last equality holds, because the projection of v is discretely harmonic on the coarse, local grid Ω_l^H. For the remaining two terms in the right hand side, we have the estimates from Sections 5.1 and 5.2. This leads to the main theorem.

Theorem 14 *Consider the LDC algorithm for the Poisson problem (21) with the following settings. Let L^H be the standard five-point discretization of the Laplacian on a uniform grid with grid sizes $\Delta x = \Delta y = H$ as in (22). Let $\Omega_l = (0,\gamma)^2$ with $0<\gamma<1$ and γ a multiple of H. Let L_l^h be the standard five-point discretization of the Laplacian on a uniform grid with grid sizes $\Delta x = \Delta y = h$ as in (47). Let $P^{h,H}$ be trigonometric interpolation. Finally, let*

$$\Omega_{def}^H = \left\{(x,y)\in\Omega_l^H \,\middle|\, x<\gamma-\epsilon \ \wedge\ y<\gamma-\epsilon\right\},$$

for some $\epsilon>0$, ϵ independent of H. Then the following upper bound for the norm of the iteration matrix M of the LDC algorithm holds:

$$\|M\|_\infty \le CH^2 + Dh^2,$$

with C, D, independent of H and h.

Proof. Let $g_\Gamma^H \in F(\Gamma^H)$. Define $\tilde{g}_\Gamma^H \in F(\Gamma^H)$ as in (70). Using (71) and Lemmas 12, 13, we find

$$\|M_2 g_\Gamma^H\|_\infty = \|M_2\tilde{g}_{\text{hor}}^H + M_2\tilde{g}_{\text{vert}}^H\|_\infty \le \left[(C_1+C_2)H^2 + (D_1+D_2)h^2\right]\|\tilde{g}_\Gamma^H\|_\infty,$$

with C_1, C_2, D_1, D_2, independent of H and h. From the definition of $\tilde{g}_\Gamma^H$, it follows that $\|\tilde{g}_\Gamma^H\|_\infty \le 2\|g_\Gamma^H\|_\infty$, and hence

$$\|M_2\|_\infty \le 2(C_1+C_2)H^2 + 2(D_1+D_2)h^2.$$

Using (25), we conclude that

$$\|M\|_\infty \le \frac{1}{4}(C_1+C_2)H^2 + \frac{1}{4}(D_1+D_2)h^2 = CH^2 + Dh^2,$$

with C, D, independent of H and h. □

6 Numerical Results

In this section, we consider the LDC algorithm described in Section 2 with the setting chosen as in Section 5, and we verify the theoretical results of Theorem 14 in some numerical experiments. For the first experiment, we apply the LDC algorithm to the boundary value problem

$$\begin{cases} -\Delta u = f, & \text{in } \Omega = (0,1)^2, \\ u = g, & \text{on } \partial\Omega. \end{cases} \tag{72}$$

In (72), f en g have been chosen such that

$$u(x,y) = \tanh\bigl[25(x+y-1/3)\bigr] + 1. \tag{73}$$

We choose a uniform, coarse grid Ω^H in Ω with grid sizes $\Delta x = \Delta y = H$ as in (22). The coarse grid discretization is the standard five-point scheme. The area of refinement Ω_l is chosen as $\Omega_l = (0,1/2)^2$. We choose a uniform, fine grid Ω_l^h in Ω_l with grid sizes $\Delta x = \Delta y = h$ as in (47). The fine grid discretization is the standard five-point scheme. Contrary to the setting in Section 5, the operator $P^{h,H}$ will be linear interpolation instead of trigonometric interpolation. The reason for this choice is that linear interpolation is more likely to be used in practice as well as shows similar convergence results. The latter will be illustrated in the second experiment.

The results of Theorem 14 hold for LDC iteration when the extent ϵ of the safety region is larger than zero and independent of H. Hence, we start by choosing $\epsilon = 1/8$, and we set

$$\Omega_{\text{def}}^H = \left\{ (x,y) \in \Omega_l^H \,\middle|\, x < 1/2 - \epsilon \ \wedge\ y < 1/2 - \epsilon \right\},$$

see Figure 3. We study the rate of convergence of the LDC algorithm for $H = 1/2^k$, $k = 3,4,\ldots$ The grid size of the local, fine grid is chosen as $h = H/2$. Numerical results are presented in Table 1(a). To demonstrate the dependence of the rate of convergence on H, we list the maximum differences δ_i, $i = 1,2,\ldots$, at the coarse grid points on the interface, viz.

$$\delta_i := \left\| u_{\Gamma,i}^H - u_{\Gamma,i-1}^H \right\|_\infty, \qquad i = 1,2,\ldots$$

and the ratios

$$\rho_i := \frac{\delta_i}{\delta_{i-1}}, \qquad i = 2,3,\ldots$$

The ratios ρ_i are nearly constant for fixed H, when they are not effected by rounding errors, and in Table 1(b), we show ρ_2 and their quotients for different grid sizes H. The ratios indicate that the rate of convergence is depending quadratically on H, as predicted by Theorem 14, indeed.

One of the main assumptions of Theorem 14 is, that the extent of the safety zone ϵ needs to be larger than zero and independent of H. Repeating the experiment with ϵ equal to zero, i.e., with no safety zone, shows that this assumption is necessary indeed. Table 2(a) lists rates of convergence for ϵ equal to zero. Although the rates of convergence are still small, implying fast convergence, they do not depend on H^2. The results seem to indicate that the rate of convergence depends on H rather than H^2. Similar results are found when we take ϵ positive, but not independent of H; Table 2(b) lists rates of convergence for $\epsilon = 2H$.

In all three Tables 1(b), 2(a,b), we used $h = H/2$. If we only change H and keep h fixed on a small value, we find similar results. This is demonstrated in Table 2(c), where we have chosen $\epsilon = 1/8$ again and where we have fixed h on $h = 1/1024$. The rates of convergence are almost the same as in Table 1(b).

Hackbusch [7, Sec. 3.2.1] and Wappler [15, Sec. 3.3.4.1] present similar numerical experiments. Both authors find the rate of convergence to depend quadratically on the coarse grid size H too, provided the extent of the safety region ϵ is larger than zero and independent of H. Wappler also studies the dependence of the rate of convergence on ϵ when ϵ depends on H linearly. His results do not show a clear convergence behavior. Wappler conjectures that the rate of convergence tends to a constant unequal to either zero or unity for H tending to zero.

Rather than applying the LDC algorithm to a specific problem and studying the rate of convergence for this specific situation, it is also possible to directly construct the iteration matrix M of Theorem 3 and calculate its norm. For the setting chosen as above, in particular linear interpolation, ϵ equal to 1/8, and $h = H/2$, we find the numerical results as in Table 3. Listed are the

H	i	δ_i	ρ_i
1/8	1	$8.66 \cdot 10^{-1}$	
	2	$2.08 \cdot 10^{-3}$	$2.41 \cdot 10^{-3}$
	3	$4.72 \cdot 10^{-6}$	$2.27 \cdot 10^{-3}$
1/16	1	$1.33 \cdot 10^{-1}$	
	2	$1.20 \cdot 10^{-4}$	$9.03 \cdot 10^{-4}$
	3	$1.04 \cdot 10^{-7}$	$8.70 \cdot 10^{-4}$
1/32	1	$2.70 \cdot 10^{-3}$	
	2	$7.55 \cdot 10^{-7}$	$2.79 \cdot 10^{-4}$
	3	$2.14 \cdot 10^{-10}$	$2.83 \cdot 10^{-4}$
1/64	1	$3.39 \cdot 10^{-4}$	
	2	$2.53 \cdot 10^{-8}$	$7.47 \cdot 10^{-5}$
	3	$1.97 \cdot 10^{-12}$	$7.79 \cdot 10^{-5}$
1/128	1	$7.16 \cdot 10^{-5}$	
	2	$1.40 \cdot 10^{-9}$	$1.95 \cdot 10^{-5}$
	3	$3.06 \cdot 10^{-14}$	$2.19 \cdot 10^{-5}$
1/256	1	$1.63 \cdot 10^{-5}$	
	2	$8.13 \cdot 10^{-11}$	$5.00 \cdot 10^{-6}$
	3	$3.11 \cdot 10^{-15}$	$3.82 \cdot 10^{-5}$
1/512	1	$3.86 \cdot 10^{-6}$	
	2	$4.87 \cdot 10^{-12}$	$1.26 \cdot 10^{-6}$
	3	$1.33 \cdot 10^{-14}$	$2.74 \cdot 10^{-3}$

(a) Maximum differences on the interface.

H	ρ_2	ratio
1/8	$2.41 \cdot 10^{-3}$	
1/16	$9.03 \cdot 10^{-4}$	0.38
1/32	$2.79 \cdot 10^{-4}$	0.31
1/64	$7.47 \cdot 10^{-5}$	0.27
1/128	$1.95 \cdot 10^{-5}$	0.26
1/256	$5.00 \cdot 10^{-6}$	0.26
1/512	$1.26 \cdot 10^{-6}$	0.25

(b) Rates of convergence.

Table 1: Rates of convergence for an H-independent safety zone ($\epsilon = 1/8$, $h = H/2$, linear interpolation).

infinity norms of the iteration matrix M from Theorem 3, and of the matrices M_1 and M_2 as defined by (24). We observe that the norm of M depends quadratically on H, which is in perfect agreement with Theorem 14. Note that we have used the upper bound 1/8 for $\|M_1\|_\infty$, cf. (25), which is not very sharp. As we are interested in the asymptotic behavior for H tending to zero, however, the matrix M_1 is not very interesting, because its norm is almost constant for decreasing H. The results of Sections 4 and 5 were targeted at estimating the norm of M_2, which depends quadratically on H indeed.

If we consider the LDC algorithm with no safety region, i.e., ϵ equal to zero, we find the results

H	ρ_2	ratio
1/8	$2.18 \cdot 10^{-2}$	
1/16	$1.12 \cdot 10^{-2}$	0.51
1/32	$1.20 \cdot 10^{-2}$	1.07
1/64	$6.78 \cdot 10^{-3}$	0.57
1/128	$3.56 \cdot 10^{-3}$	0.53
1/256	$1.79 \cdot 10^{-3}$	0.50
1/512	$8.97 \cdot 10^{-4}$	0.50

(a) No safety zone ($\epsilon = 0$, $h = H/2$).

H	ρ_2	ratio
1/8	$1.18 \cdot 10^{-4}$	
1/16	$9.03 \cdot 10^{-4}$	7.68
1/32	$8.09 \cdot 10^{-4}$	0.90
1/64	$4.31 \cdot 10^{-4}$	0.53
1/128	$2.47 \cdot 10^{-4}$	0.57
1/256	$1.02 \cdot 10^{-4}$	0.41
1/512	$3.39 \cdot 10^{-5}$	0.33

(b) Safety zone depends on H ($\epsilon = 2H$, $h = H/2$).

H	ρ_2	ratio
1/8	$2.91 \cdot 10^{-3}$	
1/16	$1.20 \cdot 10^{-3}$	0.41
1/32	$3.72 \cdot 10^{-4}$	0.31
1/64	$9.91 \cdot 10^{-5}$	0.27
1/128	$2.56 \cdot 10^{-5}$	0.26
1/256	$6.25 \cdot 10^{-6}$	0.24
1/512	$1.26 \cdot 10^{-6}$	0.20

(c) Constant grid size h ($\epsilon = 1/8$, $h = 1/1024$).

Table 2: Rates of convergence for different values of ϵ and h (linear interpolation in all tables).

H	$\|M\|_\infty$	ratio	$\|M_1\|_\infty$	ratio	$\|M_2\|_\infty$	ratio
1/8	$8.28 \cdot 10^{-3}$		$1.29 \cdot 10^{-2}$		$6.35 \cdot 10^{+0}$	
1/16	$3.82 \cdot 10^{-3}$	0.46	$1.78 \cdot 10^{-2}$	1.38	$4.35 \cdot 10^{+0}$	0.69
1/32	$1.33 \cdot 10^{-3}$	0.35	$2.04 \cdot 10^{-2}$	1.14	$2.52 \cdot 10^{+0}$	0.58
1/64	$4.01 \cdot 10^{-4}$	0.30	$2.17 \cdot 10^{-2}$	1.06	$9.33 \cdot 10^{-1}$	0.37
1/128	$1.11 \cdot 10^{-4}$	0.28	$2.23 \cdot 10^{-2}$	1.03	$2.96 \cdot 10^{-1}$	0.32

Table 3: Matrix norms for LDC iteration with an H-independent safety zone ($\epsilon = 1/8$, $h = H/2$, linear interpolation).

of Table 4. Table 4 shows that the norm of the iteration matrix increases for decreasing H, h. Hence, the rate of convergence deteriorates for smaller values of H and h. Note that the rate of convergence for the LDC algorithm with no safety region applied to boundary value problem (72) is much better than one would expect from Table 4, cf. Table 2(a).

We finally present the matrix norms for the standard experiment with $\epsilon = 1/8$ and $h = H/2$, when we use interpolation by trigonometric polynomials instead of linear interpolation. Comparing Table 3 (results for linear interpolation) and Table 5 (results for trigonometric interpolation) confirms the claim made at the beginning of this section: using linear interpolation for $P^{h,H}$ gives similar results as using trigonometric interpolation.

H	$\|M\|_\infty$	ratio	$\|M_1\|_\infty$	ratio	$\|M_2\|_\infty$	ratio
1/8	$1.64 \cdot 10^{-1}$		$1.29 \cdot 10^{-2}$		$6.93 \cdot 10^{+1}$	
1/16	$2.38 \cdot 10^{-1}$	1.45	$1.78 \cdot 10^{-2}$	1.38	$2.80 \cdot 10^{+2}$	4.03
1/32	$3.05 \cdot 10^{-1}$	1.28	$2.04 \cdot 10^{-2}$	1.14	$1.12 \cdot 10^{+3}$	4.00
1/64	$3.70 \cdot 10^{-1}$	1.21	$2.17 \cdot 10^{-2}$	1.06	$4.48 \cdot 10^{+3}$	4.00
1/128	$4.34 \cdot 10^{-1}$	1.17	$2.23 \cdot 10^{-2}$	1.03	$1.79 \cdot 10^{+4}$	4.00

Table 4: Matrix norms for LDC with no safety zone ($\epsilon = 0$, $h = H/2$, linear interpolation).

H	$\|M\|_\infty$	ratio	$\|M_1\|_\infty$	ratio	$\|M_2\|_\infty$	ratio
1/8	$8.30 \cdot 10^{-3}$		$1.29 \cdot 10^{-2}$		$6.66 \cdot 10^{+0}$	
1/16	$4.07 \cdot 10^{-3}$	0.49	$1.78 \cdot 10^{-2}$	1.38	$4.98 \cdot 10^{+0}$	0.75
1/32	$1.36 \cdot 10^{-3}$	0.33	$2.04 \cdot 10^{-2}$	1.14	$2.65 \cdot 10^{+0}$	0.53
1/64	$4.04 \cdot 10^{-4}$	0.30	$2.17 \cdot 10^{-2}$	1.06	$9.49 \cdot 10^{-1}$	0.36
1/128	$1.11 \cdot 10^{-4}$	0.27	$2.23 \cdot 10^{-2}$	1.03	$2.97 \cdot 10^{-1}$	0.31

Table 5: Matrix norms for LDC with an H-independent safety zone and trigonometric interpolation ($\epsilon = 1/8$, $h = H/2$, trigonometric interpolation).

References

[1] M. J. H. Anthonissen, B. van 't Hof, and A. A. Reusken. A finite volume scheme for solving elliptic boundary value problems on composite grids. *Computing*, 61:285–305, 1998.

[2] R. E. Ewing. Adaptive grid refinements for transient flow problems. In J. E. Flaherty, P. J. Paslow, M. S. Shephard, and J. D. Vasilakis, editors, *Adaptive Methods for Partial Differential Equations*, pages 194–205, Philadelphia, 1989. SIAM.

[3] R. E. Ewing, R. D. Lazarov, and P. S. Vassilevski. Local refinement techniques for elliptic problems on cell-centered grids. I: error analysis. *Math. Comp.*, 56:437–461, 1991.

[4] P. J. J. Ferket. *Solving Boundary Value Problems on Composite Grids with an Application to Combustion*. PhD thesis, Eindhoven University of Technology, Eindhoven, 1996.

[5] P. J. J. Ferket and A. A. Reusken. A finite difference discretization method on composite grids. *Computing*, 56:343–369, 1996.

[6] P. J. J. Ferket and A. A. Reusken. Further analysis of the local defect correction method. *Computing*, 56:117–139, 1996.

[7] W. Hackbusch. Local defect correction and domain decomposition techniques. In K. Böhmer and H. J. Stetter, editors, *Defect Correction Methods. Theory and Applications, Computing, Suppl. 5*, pages 89–113, Wien, New York, 1984. Springer.

[8] W. Hackbusch. *Elliptic Differential Equations. Theory and Numerical Treatment*. Springer, Berlin, 1992.

[9] S. McCormick. Fast adaptive composite grid (FAC) methods: Theory for the variational case. In K. Böhmer and H. J. Stetter, editors, *Defect Correction Methods. Theory and Applications, Computing, Suppl. 5*, pages 115–121, Wien, New York, 1984. Springer.

[10] S. McCormick and U. Rüde. A finite volume convergence theory for the fast adaptive composite grid methods. *Appl. Numer. Math.*, 14:91–103, 1994.

[11] S. F. McCormick. *Multilevel Adaptive Methods for Partial Differential Equations*, volume 6 of *Frontiers in Applied Mathematics*. SIAM, Philadelphia, 1989.

[12] S. F. McCormick and J. Thomas. The fast adaptive composite grid (FAC) method for elliptic equations. *Math. Comp.*, 46:439–456, 1986.

[13] H. R. Schwarz. *Numerische Mathematik*. Teubner, Stuttgart, 1986. In German.

[14] J. Thomas, R. Schweitzer, M. Heroux, S. McCormick, and A. M. Thomas. Application of the fast adaptive composite grid method to computational fluid dynamics. In *Numerical Methods in Laminar and Turbulent Flow*, pages 1071–1082, Swansea, 1987. Pineridge Press.

[15] J. U. Wappler. *Die lokale Defektkorrekturmethode zur adaptiven Diskretisierung elliptischer Differentialgleichungen mit finiten Elementen*. PhD thesis, Christian-Albrechts-Universität, Kiel, 1999. In German.